

Algorithm-based continuous pulse duration tuning and performance control of a mode-locked laser diode

N K Metzger,^{1,*} V F Olle,² A Wonfor,² R V Penty,² I H White,² M Mazilu,¹ C T A Brown,¹ and W Sibbett¹

¹*SUPA School of Physics and Astronomy, University of St Andrews, North Haugh, St Andrews, Fife, KY16 9SS, UK*

²*Electrical Division, Department of Engineering, University of Cambridge, 9 JJ Thomson Avenue, Cambridge CB30FA, UK*

*nkm2@st-andrews.ac.uk

Abstract: A control algorithm is presented that addresses the stability issues inherent to the operation of monolithic mode-locked laser diodes. It enables a continuous pulse duration tuning without any onset of Q-switching instabilities. A demonstration of the algorithm performance is presented for two radically different laser diode geometries and continuous pulse duration tuning between 0.5 ps to 2.2 ps and 1.2 ps to 10.2 ps is achieved. With practical applications in mind, this algorithm also facilitates control over performance parameters such as output power and wavelength during pulse duration tuning. The developed algorithm enables the user to harness the operational flexibility from such a laser with ‘push-button’ simplicity.

©2012 Optical Society of America

OCIS codes: (140.5960) Semiconductor lasers; (250.5960) Semiconductor lasers; (140.4050) Mode-locked lasers; (140.3425) Laser stabilization.

References and links

1. T. Ohno, K. Sato, R. Iga, Y. Kondo, I. Ito, T. Furuta, K. Yoshino, and H. Ito, “Recovery of 160 GHz optical clock from 160 Gbit/s data stream using mode locked laser diode,” *Electron. Lett.* **40**(4), 265–267 (2004).
2. P. J. Delfyett, D. H. Hartman, and S. Z. Ahmad, “Optical clock distribution using a mode-locked semiconductor-laser diode system,” *J. Lightwave Technol.* **9**(12), 1646–1649 (1991).
3. A. J. C. Vieira, P. R. Herczfeld, A. Rosen, M. Ermold, E. E. Funk, W. D. Jemison, and K. J. Williams, “A mode-locked microchip laser optical transmitter for fiber radio,” *IEEE Trans. Microw. Theory Tech.* **49**(10), 1882–1887 (2001).
4. H. Takara, “High-speed optical time-division-multiplexed signal generation,” *Opt. Quantum Electron.* **33**(7/10), 795–810 (2001).
5. D. Rachinskii, A. Vladimirov, U. Bandelow, B. Hüttl, and R. Kaiser, “Q-switching instability in a mode-locked semiconductor laser,” *J. Opt. Soc. Am. B* **23**(4), 663–670 (2006).
6. B. Hüttl, R. Kaiser, Ch. Kindel, S. Fidorra, W. Rehbein, H. Stolpe, G. Sahin, U. Bandelow, M. Radziunas, A. Vladimirov, and H. Heidrich, “Experimental investigations on the suppression of Q switching in monolithic 40 GHz mode-locked semiconductor lasers,” *Appl. Phys. Lett.* **88**(22), 221104 (2006).
7. G. Fiol, D. Arsenijevic, D. Bimberg, A. G. Vladimirov, M. Wolfrum, E. A. Viktorov, and P. Mandel, “Hybrid mode-locking in a 40 GHz monolithic quantum dot laser,” *Appl. Phys. Lett.* **96**(1), 011104 (2010).
8. M. G. Thompson, A. R. Rae, R. V. Mo Xia, R. V. Penty, and I. H. White, “Penty, and I. H. White, “InGaAs quantum-dot mode-locked laser diodes,” *IEEE J. Sel. Top. Quantum Electron.* **15**(3), 661–672 (2009).
9. S. A. Zolotovskaya, K. G. Wilcox, A. Abdolvand, D. A. Livshits, and E. U. Rafailov, “Electronically controlled pulse duration passively mode-locked Cr:forsterite laser,” *IEEE Photon. Technol. Lett.* **21**(16), 1124–1126 (2009).
10. K. A. Williams, M. G. Thompson, and I. H. White, “Long-wavelength monolithic mode-locked diode lasers,” *New J. Phys.* **6**, 179 (2004).
11. A. R. Rae, M. G. Thompson, R. V. Penty, and I. H. White, “Dynamic simulation of mode-locked quantum-dot lasers,” in *Conference on Lasers and Electro-Optics/Quantum Electronics and Laser Science Conference and Photonic Applications Systems Technologies*, OSA Technical Digest (CD) (Optical Society of America, 2008), paper CThF1.

12. M. G. Thompson, A. Rae, R. L. Sellin, C. Marinelli, R. V. Penty, I. H. White, A. R. Kovsh, S. S. Mikhlin, D. A. Livshits, and I. L. Krestnikov, "Subpicosecond high-power mode locking using flared waveguide monolithic quantum-dot lasers," *Appl. Phys. Lett.* **88**(13), 133119 (2006).
 13. C. Rulliere, in *Femtosecond Laser Pulses Principles and Experiment*, (Springer, 1998).
 14. E. A. Viktorov, P. Mandel, M. Kuntz, G. Fiol, D. Bimberg, A. G. Vladimirov, and M. Wolfrum, "Stability of the mode-locked regime in quantum dot lasers," *Appl. Phys. Lett.* **91**(23), 231116 (2007).
 15. D. Von der Linde, "Characterization of the noise in continuously operating mode locked lasers," *Appl. Phys. B* **39**(4), 201–217 (1986).
 16. U. Bandelow, M. Radziunas, A. Vladimirov, B. Hüttel, and R. Kaiser, "40 GHz mode-locked semiconductor lasers: theory, simulations and experiment," *Opt. Quantum Electron.* **38**(4-6), 495–512 (2006).
 17. J. C. Shane, M. Mazilu, W. M. Lee, and K. Dholakia, "Effect of pulse temporal shape on optical trapping and impulse transfer using ultrashort pulsed lasers," *Opt. Express* **18**(7), 7554–7568 (2010).
-

1. Introduction

Semiconductor diode lasers are of widespread interest and significance due to their high efficiency, small footprint and application-related compatibility to many sectors. In particular, monolithic mode-locked laser diodes have been studied extensively over the past two decades and are used for various optoelectronic applications that exploit their high repetition rate, low timing jitter, compactness and mechanical stability. Notable implementations have been in optical telecommunications, optical clock distribution, clock recovery, radio-over-fiber signal generation, and optical sampling [1–4]. Additionally, emerging fields such as biomedical-photonics, where typical applications are based on optical tweezing, two-photon imaging, optical coherence tomography and Raman spectroscopy, place specific demands upon the provision of compact light sources that are compatible with state-of-the-art monolithic mode-locked laser diodes (MLLD).

In contrast to ultrashort-pulse lasers based on vibronically broadened electronic transitions, MLLDs can be mode-locked by incorporating an integrated reverse-biased absorber section which gives the advantage of pulse duration adaptability as well as a facility for switching between continuous or pulsed operation via an appropriate choice of biasing parameters. It should be appreciated, however, that a laser configuration that incorporates a saturable absorber, in addition to having a stable mode locking regime can have a tendency to exhibit instabilities such as the generation of undamped Q-switched pulses [5]. In a mode-locked laser, such Q-switching instabilities lead to amplitude modulation, repetition rate variation and high jitter, all of which being undesirable in applications. The onset of such instabilities can have a major impact on device performance particularly when user control of device output over a wide parameter space is required.

The avoidance of intensity instabilities in practical devices is thus a key objective and relevant investigations have been reported by several authors where changes to physical design parameters and the use of active or hybrid mode locking has been implemented [6–8]. In a MLLD, the biasing parameters for stable and continuous pulse duration tuning must be chosen carefully and, to address this requirement, a software package has been designed and applied to provide remote and fully automated control of the operation of such a mode-locked laser. Specifically, from a graphical user interface (GUI), the operator can select the operational regime for the laser in terms of either a continuous wave (CW) output or a mode-locked regime where the duration of the pulses can be selected by the user. This development involving the direct electronic control of pulse duration is of particular interest as it enhances the operational flexibility of ultrafast diode lasers. In the field of solid-state lasers the concept of a voltage controlled saturable absorber has been implemented to achieve pulse duration changes from a minimum pulse duration of 6.4 ps by a factor of 2.7 [9]. By contrast, in this work an algorithm is used to demonstrate pulse duration tuning by a factor of 8.5 in a MLLD where the minimum pulse duration was around 1.2 ps and by a factor of 4 in a separate device where the minimum pulse duration was 520 fs. Additionally, a selectable output parameter criterion enables the MLLD to be stabilized in terms of either the output power or emission wavelength while the pulse duration is tuned.

2. Experimental setup

The mode locking performance characteristics of multi-section semiconductor laser diodes is inherently correlated to their geometric layout, the mode locking techniques used, as well as key inherent design parameters as discussed by Williams and associates [10]. In the experimental assessments described in this study, both straight- and tapered-waveguide MLLDs were used. The straight-waveguide laser is a 2-section device based on a 6 μm wide waveguide that contains a 390 μm long absorber and 1610 μm long gain section [11]. The tapered MLLD consists of a straight 500 μm long and 4 μm wide absorber section and a 1900 μm long adiabatically tapered gain section with a full taper angle of 3.4° and an aperture width of 100 μm [8,12]. The two MLLDs were investigated with the software package because their different geometry provides access to quite distinct operating regimes. In particular, with the tapered MLLD, it is possible to access shorter pulse durations due to the stronger geometrical mode confinement and thus stronger saturation in the absorber [8].

For both of the devices investigated, a passive mode locking technique for pulse generation using a reverse-biased saturable absorber section was deployed. Parameter changes in reverse bias to the absorber section and forward current to the gain section alter significantly the conditions for mode locking [8] and influence the output power, pulse duration and pulse quality such that typically the shortest pulse durations are achieved for high reverse-bias voltages associated with low drive currents. Deviations from these driving conditions lead to pulse broadening and can also give rise to deleterious undamped Q-switching.

The gain section of the lasers was biased (I_{Gain}) using an ILX laser diode driver (model: LDC 3724B), while the reverse bias (V_{Abs}) was applied using an Agilent power supply (model: E3631A). The output beam was captured in the near-field with a lensed fiber. Two fiber splitters (90:10 splitting ratio) fed the collected light into a home-built autocorrelator and a 22GHz HP radio frequency spectrum analyzer (RFSA model: 70004A). Additionally, an Agilent HP optical spectrum analyzer (OSA model: 86140A) and an Agilent power meter (model: 8153a) were linked into the fiber optical system via an additional fiber splitter (50:50 splitting ratio) to characterize the emitted light. The diode drive and light analysis setup were computer controlled using LABVIEW 8.2, the GPIB bus system and a DAQ card. A schematic of the experimental setup is shown in Fig. 1.

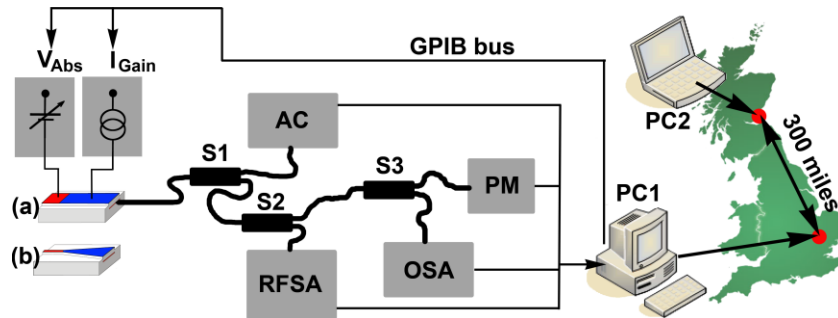


Fig. 1. Experimental setup: Mode-locked laser diode with (a) straight-waveguide and (b) tapered-waveguide. The diodes were operated via a laser diode driver (I_{Gain}) to bias the gain section and a voltage supply (V_{Abs}) to bias the absorber section of the diode. A lensed fiber picked up the emitted light field from the diode front facet. A combination of three fiber splitters (S1, S2, S3) delivered the light to an autocorrelator (AC) and a radio frequency spectrum analyzer (RFSA), an optical spectrum analyzer (OSA) and a power meter (PM). A personal computer (PC1) was used to control the setup via the GPIB bus. The computer (PC1) also served as a web server for remote access of the GUI via the internet over 500 km (over 300 miles) between Cambridge, England and St Andrews, Scotland (PC2).

3. Control algorithm

The software package designed for the pulse duration control of the laser diode consisted of a control program with a graphical user interface (GUI) and a program that generates a look-up table for the drive currents and bias voltages to create user-specified pulse durations. The GUI (shown in Fig. 2(a) and (b)) provides the user with several control features. In CW operation with the absorber section at ground potential, it is possible to alter the drive current (I_{Gain}) and change the output power only. When operated in the mode-locked regime, the user can adjust the pulse duration (τ) with a resolution of 0.01 ps. The spectral and temporal pulse shapes are then displayed and fitted automatically.

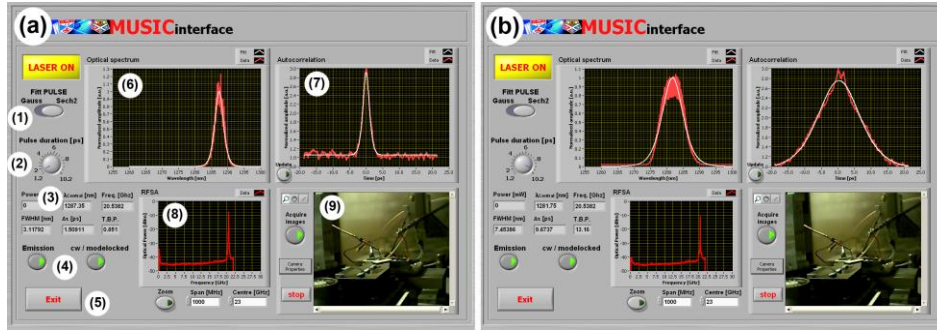


Fig. 2. The LABVIEW graphical user interface: (a) Pulse duration set to 1.5 ps. (1) Selection switch for function to be fitted (Sech²/Gaussian) (2) Pulse duration selection switch. (3) Pulse parameters: Output power [mW]; central wavelength [nm]; repetition rate [GHz]; spectral width [nm]; pulse duration [ps]; time-bandwidth product. (4) Selection switches for emission (on/off) and CW/mode-locked operation. (5) Program exit. (6) Optical spectrum with fitted function. (7) Temporal autocorrelation. (8) RFSAs trace with zoom window. (9) Experiment observation camera window. (b) Pulse duration set to 9.6 ps.

From the fitted function, the program calculates automatically the pulse duration, spectral width (at FWHM), central wavelength and time-bandwidth product [13]. Using this interface, the remote operation of the laser diode over the internet was tested using the LABVIEW web publishing tool. As shown in Fig. 1, the mode-locked laser diode could be operated via the GUI in a web browser over the 500 km (over 300 miles) between Cambridge (location of the laboratory setup and web server) and St Andrews (location of the remote GUI panel-operated web browser). In order to reduce the potential for software instabilities, this remote control is implemented as a segmented process where, unless the execution and display of a previous task is not fully completed, a new task is not begun.

To facilitate a user-defined pulse duration (τ) a look-up table is used that changes the driving parameters (I_{Gain} , V_{Abs}) of the laser diode according to the set duration. The look-up table was generated in two steps. Firstly, a map of stable mode-locked operational points of the diode was generated by varying the drive current and absorber voltage within the parameter latitude of the laser diodes. To avoid hysteresis effects [8,12] the current was set and held for one second before each measurement point at half the threshold current for the lowest reverse bias setting. This practice was proved experimentally to be sufficient to avoid hysteresis even for increasing reverse bias settings where the lasing threshold current increases as well. The mode-locked performance was assessed for each operating point before measuring the pulse duration. To determine the mode locking stability [14] and to reject unstable operational points the following two criteria based on the radio frequency spectrum analyzer (RFSAs) trace were implemented. To elucidate the effect of incomplete mode locking, three typical RFSAs traces are shown in Fig. 3(a), where two unstable or incomplete mode locking operating points are shown (blue and red). In the blue trace, a Q-switched modulated mode locking is evident as sidebands in the RFSAs trace [14] thereby causing a decreased signal-to-noise ratio (SNR) [15]. In the red RFSAs trace the decreased SNR is not

strongly evident but the observed secondary peaks at approximately 1.8 GHz off the fundamental indicate the existence of a satellite pulse thus implying imperfect mode locking [15,16]. Consequently, two separate quality criteria were implemented in the program and these are highlighted as grey areas in Fig. 3(a).

For the first criterion the RFSA trace ($P(n)$) is acquired in a window from 1 GHz to 9 GHz (Fig. 3(b)) at a resolution bandwidth of 261 kHz. Equation (1)

$$P_{RFSA} = -\sum_{n=1}^N (P(n) + P_{offset})^4 [a.u.] \quad (1)$$

is used to enhance the peaks in the measured trace, where an offset of $P_{offset} = 45$ dBm was chosen because it marks the average noise floor and RFSA signal for well-defined mode locking. N is the number of data points used from the RFSA trace. The power of 4 was chosen to enhance the value difference (P_{RFSA}) between stable and incomplete mode locking. Here odd powers were not used because they change the sign of the equation and the best results were obtained for the power of 4 given that higher values weighted the peaks in the RFSA trace excessively (see Fig. 3(b)).

A threshold of $|P_{RFSA}| < 1000$ was used to distinguish spikes in the trace originating from sub-pulsing, Q-switched mode locking as well as harmonic mode locking at half the pulse repetition rate and below. This threshold had to be determined empirically for this particular experimental setup because the noise floor (P_{offset}) of the measurement is dependent on setup parameters such as the choice of detection instruments and their settings (e.g. the resolution bandwidth of the RFSA), fiber splitters and on the fiber coupling efficiency. Small variations of the threshold at the level of $\pm 5\%$ did not affect the pulse duration tuning range of both diodes. If the threshold criterion is set too high the pulse duration tuning range for the straight-waveguide laser starts to decrease, similar when set to low the RFSA spectrum starts to show the onset of instabilities. The threshold for the straight-waveguide laser diode could be changed by up to $\pm 25\%$ without altering the tuning latitude of the pulse duration. Once the threshold was established with a reproducible fiber coupling efficiency, these values were used for the automatic evaluation of both the laser diodes mentioned here.

As a second criterion, the same threshold function was used to discern unstable mode locking and this was applied in a RFSA window between 0 and 0.5 GHz (Fig. 3(c)) with a resolution bandwidth of 10 kHz and an offset of $P_{offset} = 50$ dBm.

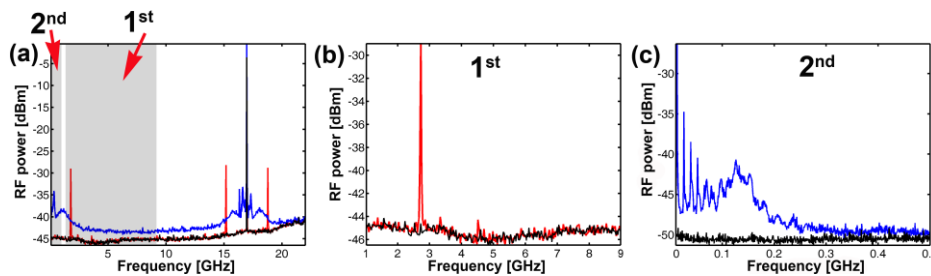


Fig. 3. (a) Three typical RFSA traces for a tapered-waveguide laser are shown from 0 to 22 GHz. Blue and red: unstable or incomplete mode-locked operation of the diode. Black: complete mode-locked operation. The windows for the first and second stability criteria are shown as grey boxes. (b) RFSA traces for first stability criterion, red is the same trace as in (a) for a frequency window from 1 to 9 GHz. The black trace indicates the RFSA floor for good mode locking at -45 dBm. (c) RFSA traces for the second stability criterion, blue is an analogous trace as in (a) at a lower resolution bandwidth in a window between 0 to 0.5 GHz. The black trace indicates the RFSA floor for good mode locking at -50 dBm.

The window width for the criteria is set automatically and depends on the pulse repetition rate of the device under investigation. The window span needs to cover more than half the fundamental repetition rate of the MLLD to capture the operational instabilities. The P_{RFSA}

graphs during pulse duration tuning are shown in Fig. 4(a) for the tapered-waveguide and (b) for the straight-waveguide lasers.

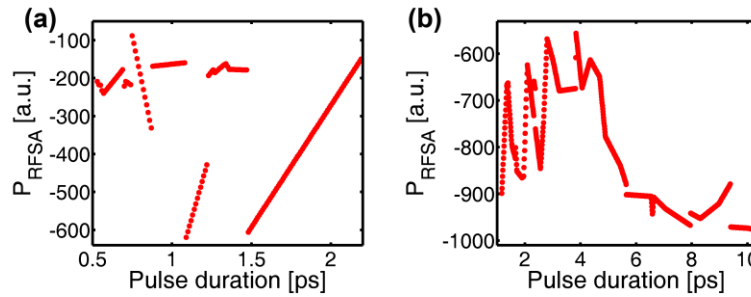


Fig. 4. (a) P_{RFSA} as a function of the pulse duration while tuning the tapered-waveguide laser from 0.52 ps to 2.19 ps. During pulse duration tuning it can be observed that the actual value (P_{RFSA}) for complete mode locking is around -600 to -250 and well in the stable regime. (b) P_{RFSA} as a function of the pulse duration while tuning the straight-waveguide MLLD from 1.17 ps to 10.19 ps. It can be seen that for the longer pulse durations (<5 ps) the value for P_{RFSA} gets close to the threshold cut off (-1000). This indicates that in this operational regime the mode locking starts to become more likely to exhibit instabilities than for shorter pulse durations. In both graphs intermediate steps were linearly interpolated from the measurement grid and verified in the reproducibility test.

Both criteria served to reject operational points of unstable mode locking and so a grid of stable driving conditions (I_{Gain} , V_{Abs}) with the associated pulse duration (τ) of the laser diode is thereby obtained. To achieve a high time resolution for the look-up table intermediate time steps were linearly interpolated in the grid data.

In the next step towards creating the look-up table, this grid data was used in a modified nearest-neighbor search algorithm. At the beginning, the algorithm determines the longest and shortest pulse durations in the measurement grid (τ_{max} , τ_{min}) where these represent respectively the start and the end point of the pulse duration look-up table. Starting at τ_{max} , the search algorithm then continuously finds the nearest neighbor with a shorter pulse duration in the grid and logs the associated diode drive parameters in the look-up table until τ_{min} is reached (see Fig. 5). This created a pulse duration look-up table $\tau(k)$ within limits τ_{max} and τ_{min} and the associated diode driving parameters $I_{\text{Gain}}(k)$ and $V_{\text{Abs}}(k)$.

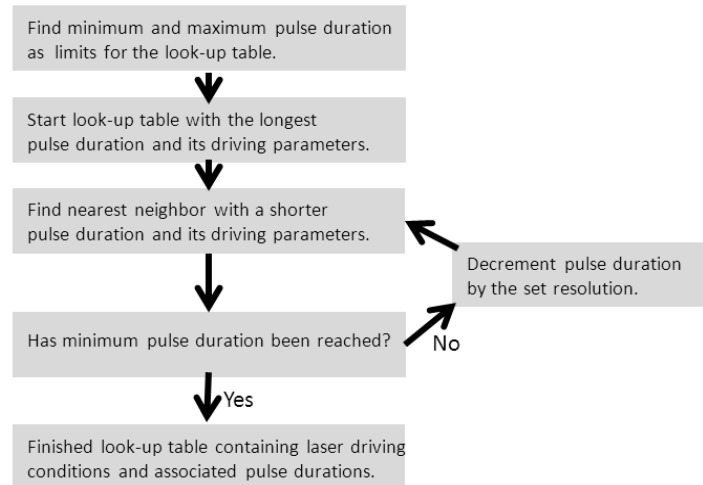


Fig. 5. Flowchart of the modified nearest-neighbor search algorithm. The algorithm creates a pulse duration look-up table $\tau(k)$ associated with the diode driving parameters ($I_{\text{Gain}}(k)$; $V_{\text{Abs}}(k)$) to facilitate continuous pulse duration tuning between τ_{max} to τ_{min} with a user defined resolution.

The nearest-neighbor search algorithm was written in MATLAB and was executed in LABVIEW via a MATLAB script node. All programs presented here could be operated in stand-alone mode or as a calibration option for the laser diode directly from the GUI front panel.

4. Results and reproducibility test

To assess the versatility of the look-up table software the two MLLD's described above were characterized automatically and the pulse duration pathway for continuous tuning determined.

In the first instance, the tapered MLLD was tested with the software and the results for the stable operation regime for the drive parameters (V_{Abs} and I_{Gain}) are shown together with the look-up table components (in red) used in the Labview GUI for continuous tuning between τ_{max} and τ_{min} in Fig. 6(a) and 6(b).

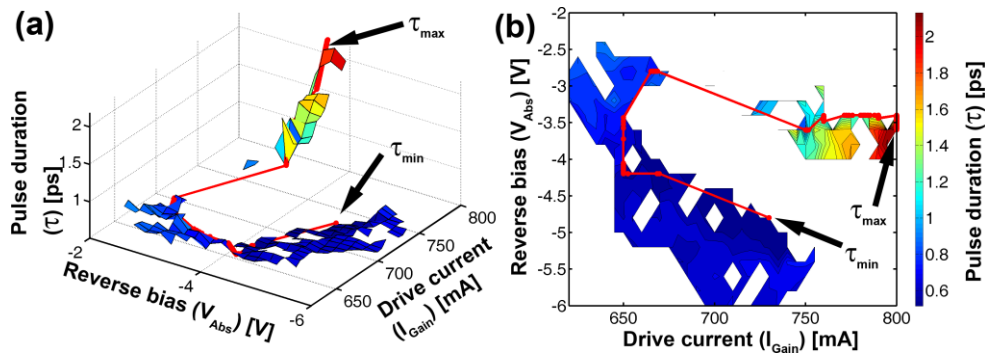


Fig. 6. (a) Tapered mode-locked laser diode look-up table components, shown in red within the stable operation regime for the driving parameters (V_{Abs} and I_{Gain}). For this diode the pulse duration could be varied from 2.19 ps down to 0.52 ps with each point marked as τ_{max} and τ_{min} respectively in the plot. (b) Top/down view of the stable operation regime.

The tapered MLLD exhibited large areas of unstable mode locking that were rejected by the stability criteria, within an overall operational regime for the drive current from 620 mA to 800 mA and absorber reverse bias from -2 V to -6 V. For this mode-locked laser diode the pulse duration could be varied from 2.19 ps down to 0.52 ps.

In a second assessment, the performance of the software was evaluated for the straight-waveguide MLLD. In contrast to the tapered laser diode, the overall operational regime was limited to drive currents from 65 mA to 150 mA but with a broader range of reverse bias settings of -4 V to -8 V. In Fig. 7(a) and 7(b) the results of the analysis are shown with drive parameters (V_{Abs} and I_{Gain}) for stable mode locking as well as the calculated look-up table (shown in red) for continuous tuning between 1.17 ps and 10.19 ps.

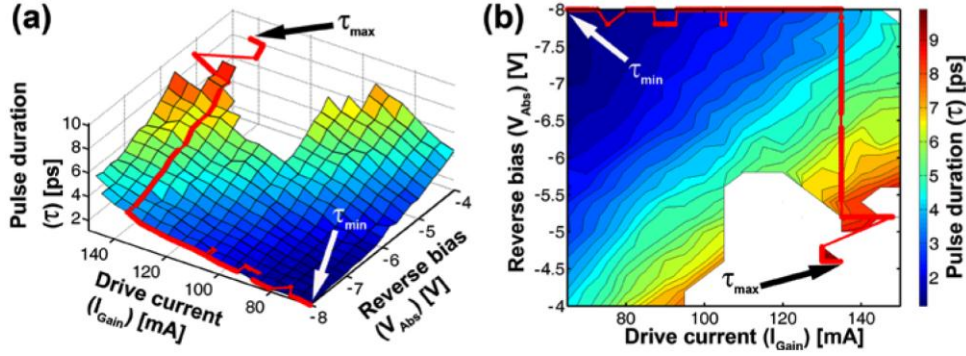


Fig. 7. (a) Road map for a straight-waveguide, mode-locked laser diode, shown in red within the stable operation regime for the driving parameters (V_{Abs} and I_{Gain}). For this diode the pulse duration could be varied from 10.19 ps down to 1.17 ps where both points are marked as τ_{max} and τ_{min} respectively in the plot. (b) Top/down view of the stable operation regime.

Both of the above figures illustrate readily the nature of the pulsed behavior for the different waveguide designs. For the straight-waveguide laser the shortest pulse durations are obtained at high reverse bias voltages and low driving currents and this observation is consistent with published data [8,11 and references therein]. Also, the typical trend of an exponentially decreasing pulse duration with linearly decreasing reverse bias where the longest pulse durations obtained for high driving currents and low reverse bias voltages is reproduced in these assessments. Importantly in this regime, effects of an absorber that is oversaturated by the circulating optical field can be observed. Here the mode locking process starts to exhibit instabilities and these operating points were consequently rejected by the algorithm.

Similar observations were made for the taper-waveguide laser, where the shortest pulse durations are obtained for high reverse bias and low driving current settings. In the work presented here an exponential-like dependence of the pulse duration as a function of reverse bias was not observed as reported in [12]. The tapered device exhibits large areas of unstable mode locking, whereas by contrast, the operation of the straight device is much more stable and less prone to mode locking instabilities.

For both designs the developed algorithm successfully generates a look-up table that serves to accomplish pulse duration tuning between the duration limits (τ_{max} and τ_{min}). For the software package used, the reproducibility of the pulse duration look-up table is also evaluated by scanning the associated driving parameters. In Fig. 8 target pulse durations or set points between 1.17 ps to 10.19 ps with step sizes of 0.5 ps are compared to measurements of the actual pulse duration achieved by the mode-locked laser diode.

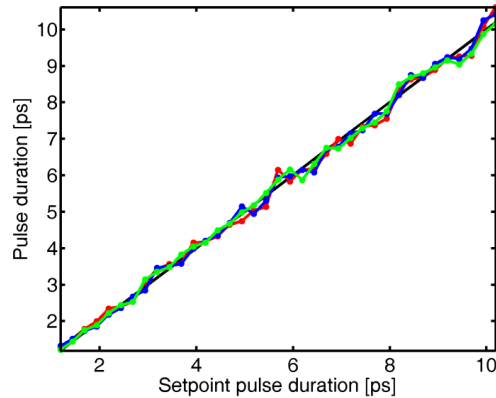


Fig. 8. Reproducibility test between 1.17 ps to 10.19 ps with set step sizes of 0.5 ps, by scanning through the calculated driving parameters and measuring the actual pulse duration over three scans (red, blue green), for the straight-waveguide MLLD.

The graphs show an accuracy of better than 7% between the set point pulse duration calculated by the algorithm (τ_{Road}) and the actual pulse duration autocorrelation measurements. It should be noted that no systematic error was observed which thus indicates a reliable operation of the software suite. The variation around the set point is attributed to the measurement inaccuracy of the autocorrelator and furthermore, drift in the free-space fiber coupling setup can cause inaccuracies during the acquisition of the autocorrelation trace. In this case, a fiber pigtailed and packaged MLLD [8] could enhance the stability and reproducibility of the results.

For mode-locked laser diodes it has to be appreciated that changing the driving parameters (drive current and reverse bias) will not only affect the pulse duration, but also other output characteristics such as average power, repetition rate, spectral width and the operational wavelength. The dependence of these output parameters on the driving conditions was also measured and the results are presented in Fig. 9(a), 9(c), 9(e) and 9(g) respectively. In everyday applications that require an adjustable pulse duration it would be highly desirable that these related outputs remain essentially constant while the pulse duration is tuned. In Fig. 9(b), 9(d), 9(f) and 9(h) the changes in these outputs were monitored for a varying pulse duration with the driving parameters determined by the algorithm.

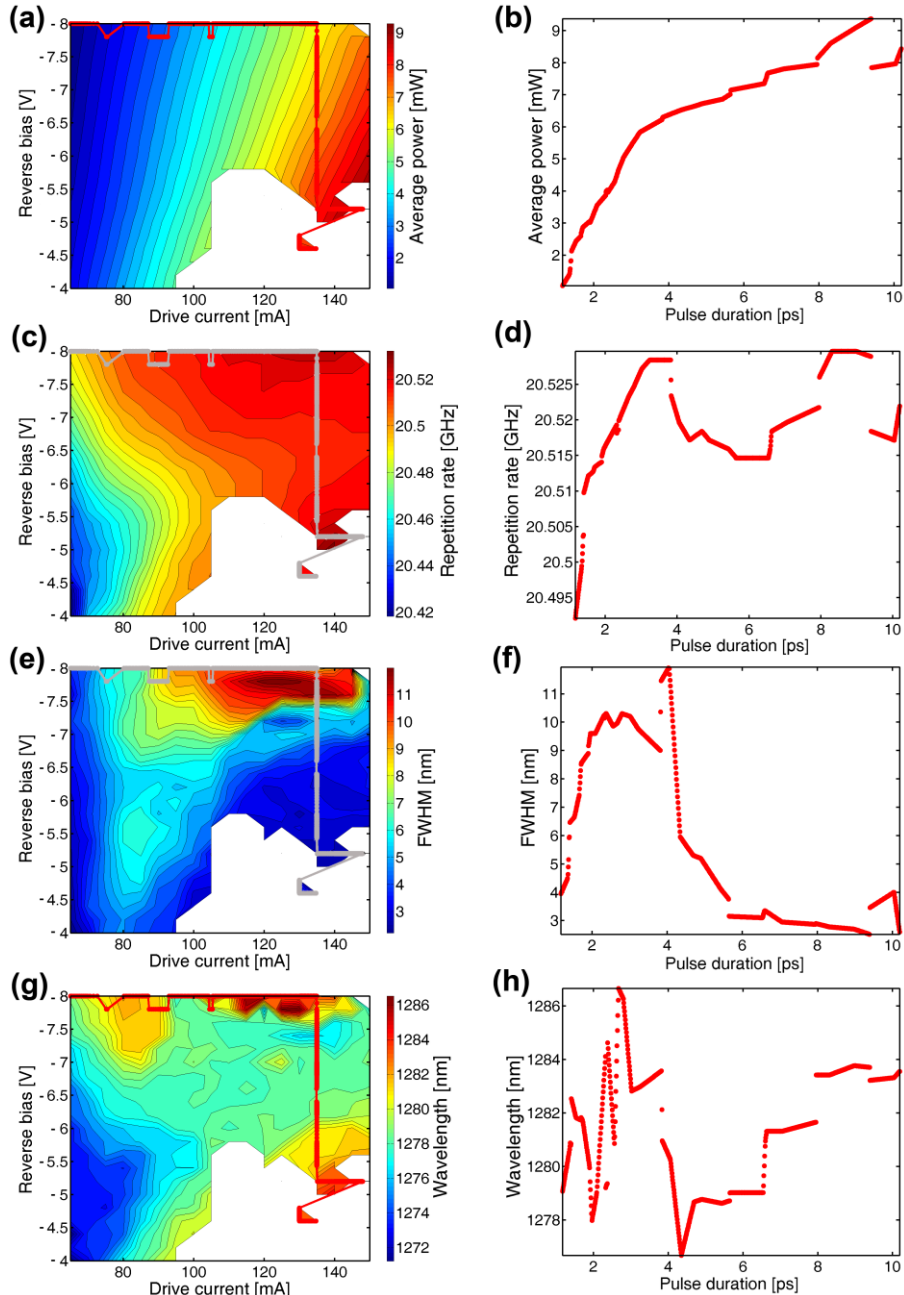


Fig. 9. Output characteristics of the straight-waveguide MLLD: (a) Average output power as a function of the drive current and reverse bias. Overlaid in red are the diode driving parameters ($I_{\text{Gain}}(k)$; $V_{\text{Abs}}(k)$) from the look-up table. (b) Laser diode average output power while the pulse duration is tuned from 1.17 ps to 10.19 ps. (c) Pulse repetition rate as a function of drive current and reverse bias. Overlaid in grey are the driving parameters from the look-up table. (d) Repetition rate during pulse duration tuning. (e) Spectral width (FWHM) of the emitted pulses as a function of the driving conditions. Overlaid in grey are the driving parameters from the look-up table. (f) FWHM during pulse duration tuning. (g) Center emission wavelength of the laser diode as a function of the driving conditions. Overlaid in red are the driving parameters from the look-up table. (h) Emission wavelength as a function of the set pulse duration. The measurement grid values for intermediate steps were again linearly interpolated as verified by the reproducibility test in Fig. 8.

While tuning the pulse duration from 1.17 to 10.19 ps the average power varies between 1 mW to 9.2 mW (Fig. 8(b)), the repetition rate varies by 20 MHz (Fig. 8(d)), the spectral width changes from 2.6 nm to 12 nm (Fig. 8(f)) and the center emission wavelength varies from 1277.2 nm to 1286.2 nm (Fig. 8(h)). As expected, these output parameter shifts are correlated with the choice of laser diode driving parameters and cannot be avoided when the complete pulse duration tuning range of the device is to be accessed. Although parameters such as the repetition rate can be deemed as minor fluctuations, the changes in output power, center wavelength and spectral width are significant. The implementation of an additional amplifier would of course eradicate the fluctuations of power with a preset amplification rate for each pulse-duration set point. However, a more desirable solution would be a purely algorithm-based approach to keep these fluctuations minimized and this option is described in the following section.

5. Control algorithm with constant laser diode output under pulse duration tuning

In this section the algorithm is modified to implement an additional constraint that keeps important output parameters closest to a target value while the pulse duration is tuned. To facilitate this supplementary criterion, the dependence of an additional output parameter (power or central wavelength; see Fig. 9(d) and (g)) on the driving parameters (I_{Gain} , V_{Abs}) was logged during the acquisition of the map of stable mode-locked operational points. As discussed previously in the unconstrained algorithm, it starts at τ_{max} and finds all points in the map of stable mode locking that have a shorter pulse duration. Their respective driving parameters are logged and all output values retrieved for these driving conditions from the output parameter map. In a subsequent step the new algorithm searches for the output parameter that is closest to a predefined target value. The driving conditions for this output parameter define the new point on the road map for pulse duration tuning and are saved in the look-up table. Notably the predefined target output value can be a preferred wavelength of operation or output power of the laser diode desired by the user. However, to achieve the broadest pulse duration tuning range of the diode, this value was automatically set to the peak of the histogram function of all output values and serves as another defining constraint for the algorithm.

With this approach, the pulse duration look-up table $\tau(k)$ within limits τ_{max} and τ_{min} contains the associated diode driving parameters $I_{\text{Gain}}(k)$ and $V_{\text{Abs}}(k)$ where the selected constrained output parameter is held closest to a target value. The associated flowchart of this algorithm is depicted in Fig. 10, where the additional constraint decision is marked in red.

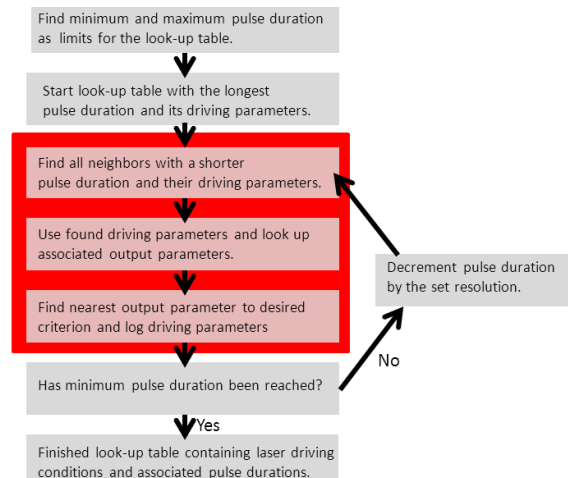


Fig. 10. Flowchart of the constrained nearest-neighbor search algorithm. The algorithm creates a pulse duration look-up table $\tau(k)$ associated with the diode driving parameters ($I_{\text{Gain}}(k)$; $V_{\text{Abs}}(k)$) to facilitate continuous pulse duration tuning between τ_{max} to τ_{min} while keeping an desired laser diode output parameter nearest to a target value. [The additional output constraint criterion is marked in red.]

To illustrate the function of the constrained search algorithm and for comparison with the results of the unconstrained algorithm the MLLD output power and center emission wavelength were chosen as an additional constrained parameter and the results are shown in Fig. 11(a) and (c) respectively.

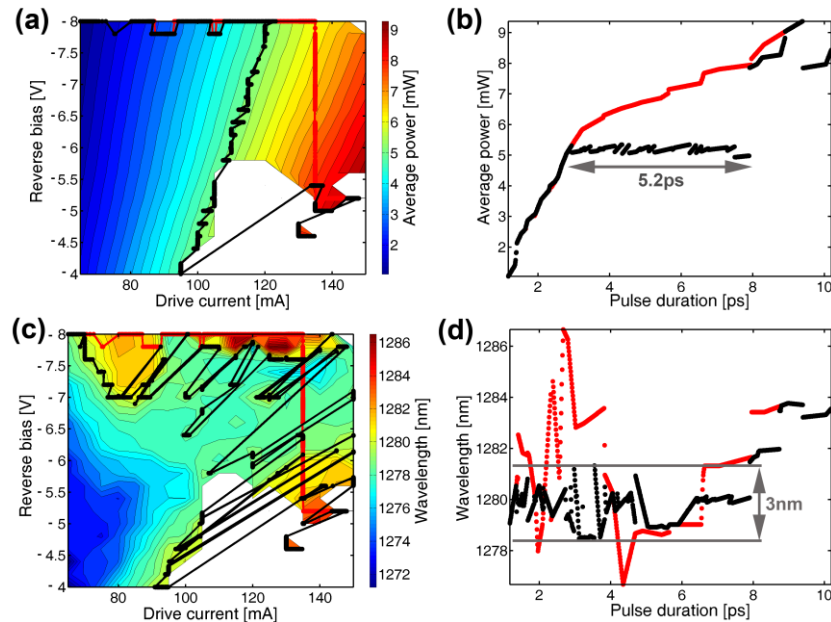


Fig. 11. (a) Black line: road map for a straight-waveguide, mode-locked laser diode, when an 5.2 mW output power constraint is used. The false color plot shows the average output power within the stable operation regime for the driving parameters (V_{Abs} and I_{Gain}). Additionally the unconstrained road map is plotted as a red line. (b) Variation of the output power as a function of the pulse duration set points (1.17 ps to 10.19 ps) for the constrained algorithm (black line) and unconstrained algorithm (red line). (c) Black line: road map for a straight-waveguide MLLD, when an 1280 nm output wavelength constraint is used. The false color shows the emission wavelength within the stable operation regime for different driving parameters. Additionally the unconstrained road map is plotted as a red line. (d) Variation of the emission wavelength as a function of the pulse duration set points (1.17 ps to 10.19 ps) for the constrained algorithm (black line) and unconstrained algorithm (red line). The measurement grid values for intermediate steps were linearly interpolated and are verified through the reproducibility test in Fig. 8.

From Fig. 11(b) it can be seen that even with an additional power constraint the power fluctuates over 8.2 mW. However, if the tuning range is restricted to the latitude of 2.8 ps to 8 ps the power fluctuations are smaller than 0.2 mW. A similar behavior is observed for the center wavelength constraint (Fig. 11(d)) where the fluctuations can be confined to 3 nm when the pulse duration tuning range is limited from 1.17 ps to 8 ps.

6. Discussion and conclusion

The software package outlined in this study enables a fully integrated and automated control to be implemented for a mode-locked diode laser via a single graphical user interface (GUI). Importantly, linear and stable tuning of the pulse duration was realized by means of an algorithm that extracted a look-up table for stable mode locking. The functionality of the algorithm was tested on two MLLD's with different stability and pulse duration characteristics and the software was shown to facilitate precise adjustment of pulse durations by users at the turn of a dial [17]. Furthermore, the possibility to constrain output parameter fluctuations during pulse duration tuning by including an additional selection criterion was investigated. Fluctuations in output power and center emission wavelength were restrained when part of the pulse duration tuning range was sacrificed.

This approach enables stand-alone operation without expensive diagnostic tools facilitated through the look-up table. Together with the remote control capability of the system via the internet, it enables the user to operate the system in hazardous remote or hard to access environments for example in clean rooms. Thus, this completely algorithm-based approach to enhancing the versatility of mode-locked lasers could have major implications on the uptake of such lasers for a wider range of users in both the research and industrial sectors.

Acknowledgements

Funding for this research was provided by the UK Engineering and Physical Sciences Research Council in a project entitled Ultrafast Modular Lasers. We acknowledge the supply of the quantum-dot material for the laser samples by Dr A Kovsh of Innolume GmbH.